Weak- and strong-field dynamos: from the Earth to the stars

J. Morin, E. Dormy, M. Schrinner, J. -F. Donati

Monthly Notices of the ROYAL ASTRONOMICAL SOCIETY LETTERS

Mon. Not. R. Astron. Soc. **418,** L133–L137 (2011) doi:10.1111/j.1745-3933.2011.01159.x

Weak- and strong-field dynamos: from the Earth to the stars

J. Morin,[1★] E. Dormy,[2] M. Schrinner[2] and J.-F. Donati[3]

[1]*Dublin Institute for Advanced Studies, School of Cosmic Physics, 31 Fitzwilliam Place, Dublin 2, Ireland*
[2]*MAG (ENS/IPGP), LRA, Ecole Normale Supérieure, 24 Rue Lhomond, 75252 Paris Cedex 05, France*
[3]*IRAP-UMR 5277, CNRS & Univ. de Toulouse, 14 Av. E. Belin, F-31400 Toulouse, France*

Accepted 2011 September 13. Received 2011 August 24; in original form 2011 June 21

ABSTRACT

Observations of magnetism in very low mass stars recently made important progress, revealing characteristics that are now to be understood in the framework of dynamo theory. In parallel, there is growing evidence that dynamo processes in these stars share many similarities with planetary dynamos. We investigate the extent to which the weak-field *versus* strong-field bistability predicted for the geodynamo can apply to recent observations of two groups of very low mass fully-convective stars sharing similar stellar parameters but generating radically different types of magnetic fields. Our analysis is based on previously published spectropolarimetric and spectroscopic data. We argue that these can be interpreted in the framework of weak- and strong-field dynamos.

Key words: dynamo – planets and satellites: magnetic fields – stars: low-mass – stars: magnetic field.

1 INTRODUCTION

Many stars possessing an outer convective envelope – like the Sun – exhibit a variety of activity phenomena (e.g. cool spots producing photometric variations, a hot corona detected at radio and X-ray wavelengths) powered by their magnetic field. The latter is generated by dynamo processes converting kinetic energy (due to thermal convection) into magnetic energy. In the Sun, and other solar-type stars, the tachocline, a thin shear layer at the base of the solar convection zone, is thought to play an important role in generating the magnetic field (e.g. Charbonneau & MacGregor 1997). On the contrary, main-sequence stars below $0.35\,M_\odot$ being fully convective do not possess a tachocline. Dynamo processes in these objects are therefore believed to differ significantly from those in the Sun; in particular, they may operate throughout the whole stellar interior (e.g. Chabrier & Küker 2006; Browning 2008).

Measurements of surface magnetic fields on a number of M dwarfs ($0.08 < M_\star/M_\odot < 0.7$) have recently been available using two complementary approaches. One is based on spectroscopy: the average value of the scalar magnetic field at the surface of the star is inferred from the analysis of the Zeeman broadening of spectral lines (Saar 1988; Reiners & Basri 2006). The other approach uses time-series of circularly polarized spectra and tomographic imaging techniques to produce spatially resolved maps of the large-scale component (typically up to spherical harmonic degree ℓ_{max} in the range 6–30, depending on the rotational velocity) of the vector magnetic field (Zeeman–Doppler Imaging, hereinafter ZDI, Semel 1989; Donati & Brown 1997; Donati et al. 2006b). We refer to Morin et al. (2010b) and references therein for a more detailed comparison. The first spectropolarimetric observations of a fully-convective M dwarf (V374 Peg, Donati et al. 2006a; Morin et al. 2008a) have revealed that these objects can host magnetic fields featuring a long-lived strong dipolar component almost aligned with the rotation axis, much more reminiscent of planetary magnetic fields than those observed in the Sun or solar-type stars (e.g. Donati et al. 2003).

Despite many differences between planetary and stellar interiors, a few recent studies have strengthened the idea that some fundamental properties of stellar dynamos could be captured by simple Boussinesq models (i.e. without taking into account the radial dependency of the stellar density). An accurate description of the interior dynamics of stars requires considering their density stratification. This can be more reliably achieved by anelastic models. It seems, however, that some characteristics are robust enough to be already captured by a Boussinesq description. Goudard & Dormy (2008) have shown, for one given set of parameters, that numerical simulations in the Boussinesq approximation can reproduce some basic characteristics of either the magnetism of planets or partly-convective stars – steady axial dipole versus cyclic dynamo waves, respectively – by varying a single parameter: the relative width of the convection zone (a thin shell leads to dynamo waves). (Christensen, Holzwarth & Reiners 2009, hereinafter C09) showed that a scaling law for the magnetic field strength originally derived from a large number of Boussinesq geodynamo simulations is also applicable to rapidly rotating, fully-convective stars (either main-sequence M dwarfs or young contracting T Tauri stars).

Featherstone et al. (2009) show that dynamo action in a fully-convective sphere (simulating the core of a A-type star) can be strongly enhanced by using a strong initial dipolar field, as in

★E-mail: jmorin@cp.dias.ie

contrast to the case where only a small seed field is initially present. The dipolar solution bears strong similarities with Boussinesq geodynamo models, as noted by the authors. Moreover, the existence of two coexisting solutions for a given parameter set seems to be reminiscent of the bistability described in Simitev & Busse (2009) and found in Boussinesq models.

Recent spectropolarimetric observations by Morin et al. (2010a, hereinafter M10a) have revealed two radically different types of large-scale magnetism for M dwarfs with similar masses and rotation periods. One possible explanation for these observations could be the existence of two dynamo branches in this parameter regime. In this Letter, we briefly summarize the observational results on fully-convective stars, describe the theoretical framework of the weak-field *versus* strong-field dynamo bistability, and discuss its applicability to very low mass stars.

2 LARGE-SCALE VERSUS TOTAL MAGNETIC FIELD

Following the study of V374 Peg, a first spectropolarimetric multi-epoch survey was initiated for a sample of 23 active M dwarfs. The survey intended to constrain the effects of the shift towards a fully-convective internal structure on dynamo action (Donati et al. 2008; Morin et al. 2008b; M10a) by mapping the large-scale component of the surface magnetic field and assessing the corresponding magnetic flux (with a typical uncertainty of the order of 20 per cent).[1]

All the fully-convective stars of the sample lie in the so-called saturated dynamo regime – corresponding to $P_{\rm rot} \lesssim \{5, 10\}$ d for a $\{0.35, 0.15\}$ M$_\odot$ star (see Kiraga & Stepien 2007; Reiners, Basri & Browning 2009). In this regime, the rapid dependence of the magnetic flux on the rotation rate observed for slower rotators (Rossby numbers larger than 0.1) suddenly stops. The observations (in terms of X-ray activity or Zeeman broadening) are consistent with a magnetic field almost independent of the rotation rate. We will come back to this point in Section 4. We indeed verified that for stars for which such measurements exist, the total magnetic flux inferred from unpolarized spectra is in the range of 1–4 kG (i.e. matching the C09 scaling law). Two radically different types of large-scale magnetic fields are observed, either a strong and steady axial dipole field (hereinafter SD) or a weaker multipolar, non-axisymmetric field configuration in rapid evolution (hereinafter WM), whereas no distinction between these two groups of stars can be made on the basis of mass and rotation only (see Fig. 1).

All stars in the strong dipole regime have a typical large-scale magnetic flux of 1 kG (values comprised between 0.5 and 1.6 kG), whereas for those in the weak, multipolar regime, the typical value is 0.1 kG (all values are lower than 0.2 kG) and it is much more variable for a given object. The latter is only found in the parameter ranges $M_\star < 0.15$ M$_\odot$ and $P_{\rm rot} < 1.5$ d in our sample, though the limits of the domain in which this behaviour occurs are not yet well defined (see Figs 1 and 2); additional observations on a larger sample of very low mass stars are needed to specify this point.

Measurements of the total magnetic flux $B_{\rm I}$ from unpolarized spectroscopy are available for a number of stars in our spectropolarimetric sample (see Fig. 3), with typical uncertainties in the range 0.5–1 kG (Reiners et al. 2009; Reiners & Basri 2010). The three objects featuring $B_{\rm I} \sim 4$ kG are in the SD regime – large red decagons – but both SD and WM large-scale magnetic fields are

[1] Here we term the average modulus of the surface magnetic field 'magnetic flux' (see Reiners 2010 for a discussion on this term).

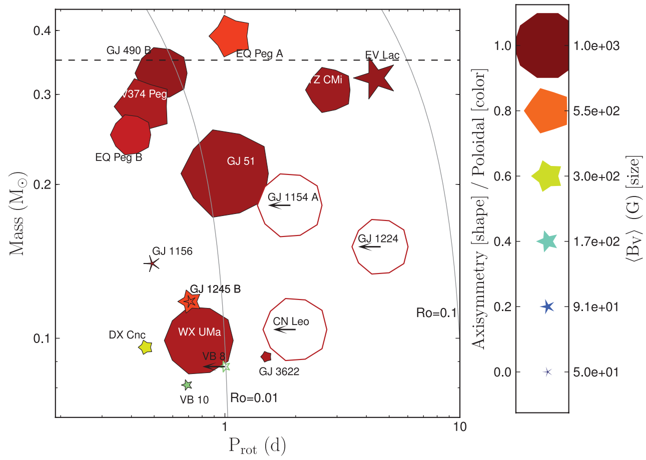

Figure 1. Mass–period diagram of fully-convective stars derived from spectropolarimetric data and ZDI by Morin et al. (2008b), Phan-Bao et al. (2009) and M10a. The symbol size represents the reconstructed magnetic energy, the colour ranges from blue to red for purely toroidal to purely poloidal field, and the shape depicts the degree of axisymmetry from a sharp star for non-axisymmetric to a regular decagon for axisymmetric. For a few stars of the sample, M10a could not perform a definite ZDI reconstruction; in these cases, only an upper limit of the rotation period is known and the magnetic flux is extrapolated; those objects are depicted as the empty symbols. The theoretical fully-convective limit is depicted as the horizontal dashed line. The thin solid lines represent contours of constant Rossby number Ro = 0.01 (left-hand side) and 0.1 (right-hand side), as estimated in M10a.

found among the stars having $B_{\rm I} \sim 2$ kG (see Fig. 3). We therefore conclude that there is no systematic correlation between the unpolarized magnetic flux $B_{\rm I}$ and the large-scale magnetic topology inferred from spectropolarimetric observations. Hence, the two different types of magnetic field configurations are only detected when considering the large-scale component (probed by spectropolarimetry, and which represents 15–30 per cent of the total flux in the SD regime, but only a few per cent in the WM regime) and not the total magnetic flux derived from unpolarized spectroscopy.

3 WEAK- AND STRONG-FIELD DYNAMOS

It has been known since Chandrasekhar (1961) that both, magnetic fields and rotation, taken separately tend to inhibit convective motions, but that if both effects are combined, then the impeding influences of the Lorentz and the Coriolis forces may be partly relaxed, allowing convection to set in at lower Rayleigh number and to develop on larger length-scales (see also Eltayeb & Roberts 1970). This mutual counteraction of rotation and magnetism is most effective in the magnetostrophic regime, i.e. if the Lorentz and Coriolis forces are of the same order of magnitude (see Chandrasekhar 1961; Soward 1979; Stevenson 1979). This led Roberts (1978) to conjecture the existence of two different dynamo regimes – a weak- and a strong-field branch – and that these different dynamo solutions could coexist over some range of parameters (see also Roberts 1988, for a review). The anticipated bifurcation diagram (adapted from Roberts 1988) is presented in Fig. 4. For dynamos belonging to the weak-field branch, the Proudman–Taylor constraint can only be broken owing to the presence of the viscous or the inertial term in the momentum equation. This weak-field force balance requires small length-scales. In the strong-field branch, however, the Lorentz force relaxes the rotational constraint. A similar bifurcation

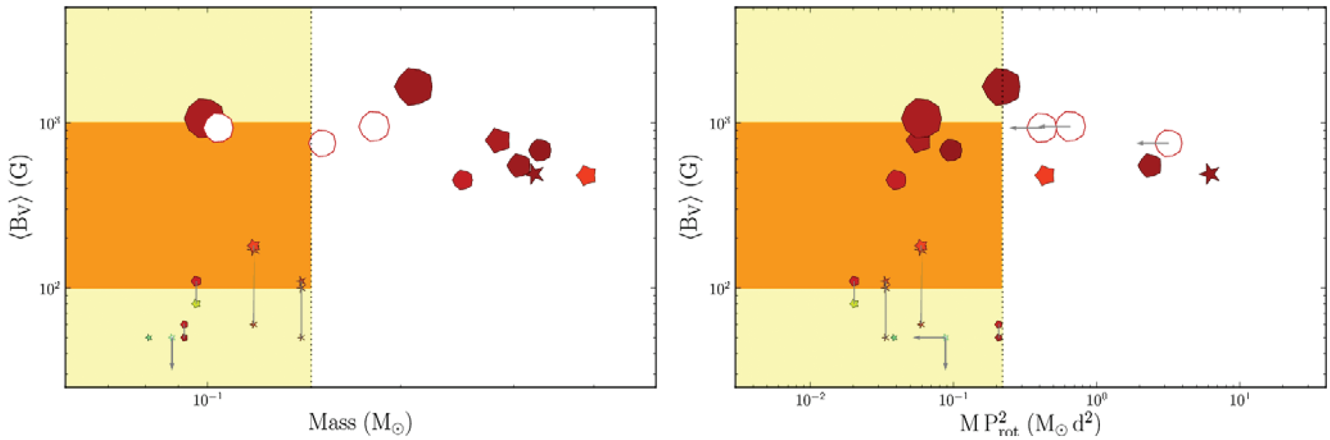

Figure 2. Average large-scale magnetic fluxes of fully-convective stars derived from spectropolarimetric data and ZDI, as a function of mass (left-hand panel) and mass × $P_{\rm rot}^2$ (right-hand panel). The symbols are similar to those used in the mass–period diagram (see Fig. 1). For stars in the WM regime, the symbols corresponding to different epochs for a given star are connected by the vertical grey line. The yellow region represents the domain where bistability is observed and the orange one separates the two types of magnetic fields identified (see text).

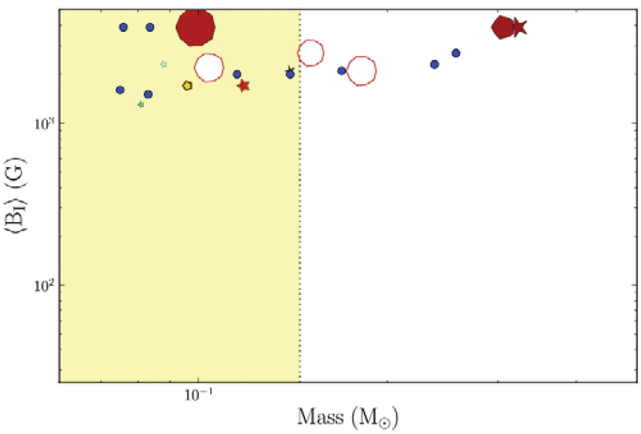

Figure 3. Total magnetic fluxes of fully-convective stars in the saturated regime measured from unpolarized spectra of Fe H lines. The values are taken from Reiners et al. (2009) and Reiners & Basri (2010), whenever 2MASS near-infrared luminosities (Cutri et al. 2003) and *Hipparcos* parallaxes (ESA 1997) are available to compute the stellar mass from the Delfosse et al. (2000) mass–luminosity relation. Whenever spectropolarimetric data are available, the properties of the magnetic topology are represented by the symbols described in Fig. 1. The magnetic field (y-axis) scale is the same as in Fig. 2. The yellow region represents the mass domain where bistability is observed in spectropolarimetric data (see Fig. 2).

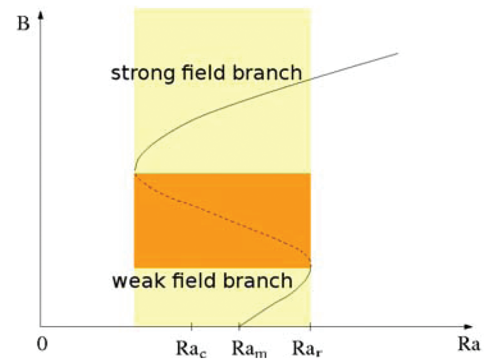

Figure 4. Anticipated bifurcation diagram for the geodynamo (adapted from Roberts 1988). The magnetic field amplitude is plotted against the Rayleigh number. The bifurcation sequence is characterized by two branches, referred to as weak- and strong-field branches. The yellow and orange regions have the same meaning as in Fig. 2. $Ra_{\rm c}$ is the critical Rayleigh number for the onset of non-magnetic convection. The weak-field regime sets in at $Ra_{\rm m}$, and the turning point associated with the runaway growth corresponds to $Ra = Ra_{\rm r}$.

diagram, but based on the fact that magnetic buoyancy would be negligible close to the dynamo onset, has been proposed for stars by Weiss & Tobias (2000).

The existence of a strong-field dynamo regime has received support from theoretical and numerical studies (e.g. Childress & Soward 1972; Fautrelle & Childress 1982; St. Pierre 1993). More recently, numerical simulations have supported the existence of both branches in spherical geometry, that is, both weak- and strong-field solutions were obtained depending on the initial conditions (Dormy E. & Morin V., in preparation).

4 DISCUSSION

We now speculate that the group of stars showing multipolar and time-varying magnetic topologies (WM) correspond to the weak-field regime, whereas those with a steady dipole (SD) belong to the strong-field branch.

The usual control parameter in the weak-field *versus* strong-field dynamo scenario described above is the Rayleigh number, which measures the energy input relative to forces opposing the motion. Mass can be used as a good proxy for the available energy flux in M dwarfs. Fig. 2(a) can therefore be interpreted as a bifurcation diagram for the amplitude of the large-scale magnetic field versus a control parameter measuring the energy input. In order to compare the driving of convection with the impeding effect of rotation, we can use $M P_{\rm rot}^2$ as a rough proxy for the Rayleigh number (see Fig. 2b) based on rotation rather than diffusivities (e.g. Christensen & Aubert 2006).

Such an identification implies that (i) the strong-field–weak-field dichotomy only affects the large-scale component of the magnetic field; and (ii) the field strength is compatible with a Lorentz-inertia force balance for stars featuring a WM magnetism, whereas a Lorentz–Coriolis balance prevails for stars in the SD group. It is difficult to quantify the range of control parameters over which both branches coexist; we will therefore focus our discussion on the prevailing force balances in both regimes and their implications on the magnetic field.

4.1 Large-scale dynamo bistability

Different types of magnetism have previously been found to affect only the large-scale component of the magnetic field (measured with spectropolarimetry) and not the total magnetic flux (measured with unpolarized spectroscopy). Indeed, the aforementioned spectropolarimetric survey has revealed that the large-scale magnetic field of M dwarfs rapidly changes with stellar mass (both in geometry and field strength) close to the fully-convective limit (Donati et al. 2008; Morin et al. 2008b), whereas no change is visible in total magnetic flux measurements (Reiners & Basri 2007). As the large-scale component only represents a small fraction of the total flux, a change affecting the large-scale field alone can indeed remain unnoticed in the measured values of the total field.

The Rossby number in stars is much higher than in the Earth's interior and associated with a stronger driving. Therefore, whereas the geodynamo must act on comparatively larger scales (because of the fairly moderate value of the magnetic Reynolds number), motions in stellar interiors most likely generate fields on a variety of scales, which includes the possible coexistence of a large-scale dynamo with a small-scale dynamo (Vögler & Schüssler 2007; Cattaneo & Hughes 2009) . Such coexistence could easily account for the difference in measurements provided by spectropolarimetry (Fig. 2) and unpolarized spectra (Fig. 3).

4.2 Force balance and magnetic field strength

In the strong-field regime, the Lorentz and Coriolis forces are of the same order of magnitude. The ratio of the two forces can be estimated by the Elsasser number

$$\Lambda = \frac{B^2}{\rho\mu\eta\Omega}, \tag{1}$$

where B is the magnetic field strength, ρ is the mass density, μ is the magnetic permeability, η is the magnetic diffusivity and Ω is the rotation rate.

This magnetostrophic force balance is valid for large spatial scales which are strongly affected by the Coriolis force, and does not apply to small spatial scales for which the inertial term is predominant in the momentum equation. It is important to note here that the Elsasser number only provides a crude measurement for this force balance. To establish this measure, an equilibrium between induction and diffusion is assumed in the induction equation. In doing so, the typical length-scales of the field and of the flow have to be considered equal. While this is a sensible approximation for a planetary dynamo working at a moderate magnetic Reynolds number, it is a crude approximation for stellar interiors. More importantly, this force balance can only provide an order of magnitude estimate for the field strength. The magnetic energy in the strong-field branch will obviously vary with the amount of thermal energy available (see Fig. 4 and Roberts 1988). Let us nevertheless try to provide an estimate of the surface field corresponding to an Elsasser number of unity for M dwarfs. We simply take $\rho = M_\star/(\frac{4}{3}\pi R_\star^3)$, and similarly to C09, we assume that the ratio between the magnetic field inside the dynamo region and the surface value is equal to 3.5. An estimate for the turbulent magnetic diffusivity is also required; crude values, which can be derived from the sunspot or active regions' decay time or from the formula $\eta \sim u_{\rm rms}\ell$ (where $u_{\rm rms}$ is the turbulent velocity and ℓ is a typical length-scale), are in the range 10^{11}–3×10^{12} cm^2 s^{-1} (e.g. Rüdiger, Kitchatinov & Brandenburg 2011) . Let us introduce $\eta_{\rm ref} \equiv 10^{11}$ cm^2 s^{-1}. With $\eta \propto u_{\rm rms}\ell$, assuming that $u_{\rm rms}$ scales with $L_\star^{1/3}$ according to mixing-length theory (Vitense 1953), and ℓ with the depth of the convective zone, we derive an estimate of the field strength at the stellar surface in the strong-field regime:

$$B_{\rm sf} \sim 6 \left(\frac{M_\star}{\rm M_\odot}\right)^{1/2} \left(\frac{R_\star}{\rm R_\odot}\right)^{-1} \left(\frac{L_\star}{\rm L_\odot}\right)^{1/6} \times \left(\frac{\eta_\odot}{\eta_{\rm ref}}\right)^{\mathbf{1/2}} \left(\frac{P_{\rm rot}}{1\,{\rm d}}\right)^{-1/2} \;{\rm kG}. \tag{2}$$

Taking the stellar radius and luminosity for the stellar mass in the range 0.08–0.35 $\rm M_\odot$ from Chabrier & Baraffe (1997) main-sequence models, we note that $B_{\rm sf}$ is almost independent of mass in this range, and thus the main dependence is on the rotation period and the chosen reference magnetic diffusivity $\eta_\odot$.

However, we do not find evidence for a dependence of the large-scale magnetic flux on the rotation period among stars belonging to the strong-field branch in the spectropolarimetric data. Depending on the precise extent of the bistable domain, a factor of 2–3 in magnetic fluxes would be expected between the fastest and slowest rotators of our sample. Such a moderate dependence might remain undetected due to the dispersion (object-to-object variations) of measurements. Using the aforementioned estimate of $\eta_\odot$ and the rotation periods of the stars in the spectropolarimetric sample, we find surface values in the strong-field regime ranging from 2 to 50 kG. Such estimates are compatible with the order of magnitude of the measured large-scale magnetic fluxes. It should be stressed, however, that this is not conclusive as the weak-field branch is only a factor of 10 smaller in magnitude.

The weak-field *versus* strong-field scenario can, however, receive additional support by considering the ratio between field strengths in the weak- and strong-field regimes (i.e. the amplitude of the gap between both branches). In the case of the Earth's core, inertia and viscous terms become significant at a similar length-scale [because $Ro^2 E^{-1} \sim \mathcal{O}(1)$]. In stellar interiors, however, the Rossby number is usually much larger than in the Earth's core (by a factor of at least 10^4). A weak-field branch would therefore naturally result from a balance between Lorentz and inertial forces through the Reynolds stresses (i.e. the field strength in the weak-field branch should approach equipartition between kinetic and magnetic energies). Therefore, the ratio between field strengths in the weak- and strong-field regimes – corresponding to a different force balance – is expected to depend on the ratio between inertia and Coriolis forces. We can thus estimate

$$\frac{B_{\rm wf}}{B_{\rm sf}} = Ro^{1/2}, \tag{3}$$

where Ro is the Rossby number. M10a derived empirical Rossby numbers of the order of 10^{-2} for stars in the bistable domain, implying a ratio $B_{\rm sf}/B_{\rm wf}$ of the order of 10, which is indeed the typical ratio between large-scale magnetic fields measured in the WM and SD groups of stars (see Fig. 2 and Section 2).

We shall now discuss an apparent caveat of the proposed scenario. As noted in Section 2, all the stars considered in our sample belong to the so-called *saturated regime* (Kiraga & Stepien 2007; Reiners et al. 2009). This means that the strong variation of the field strength with $P_{\rm rot}$ observed for lower rotation rates has 'saturated' and the amplitude of the field seems to be independent of the rotation rate of the star. Hence, there is an apparent contradiction to the possibility of a strong-field branch, in which the magnetic field depends on the rotation rate as $B_{\rm sf} \propto \Omega^{1/2}$. The first important point is that $B_{\rm sf} \propto \Omega^{1/2}$ (derived from $\Lambda \sim 1$) should apply here to the large-scale field alone, which is only a fraction of the total magnetic field of the stars (between 15 and 30 per cent). If a small-scale dynamo operates, it does not need to follow the same dependency. Besides, the slope of this flat portion of the rotation–magnetic field relation (either of the overall magnetic flux based on unpolarized spectroscopy or of its proxy, the relative X-ray luminosity L_X/L_{bol}) is poorly constrained in the fully-convective regime and is in fact compatible with a $\Omega^{1/2}$ dependence. Evidence for such a dependence of the large-scale magnetic field on $\Omega^{1/2}$ would strongly support the proposed scenario.

5 CONCLUSION

In this Letter, we compare the bistability predicted for the geodynamo with the latest results on spectropolarimetric observations of fully-convective main-sequence stars (M10a). We show that the weak-field *versus* strong-field dynamo bistability is a promising framework to explain the coexistence of two different types of large-scale magnetism in very low mass stars. The order of magnitude of the observed magnetic field in stars hosting a strong dipolar field (SD), and more conclusively the typical ratio between large-scale magnetic fields measured in the WM and SD groups of stars, is compatible with theoretical expectations. We argue that the weak dependency of the magnetic field on stellar rotation predicted for stars in the strong-field regime cannot be ruled out by existing data and should be further investigated. We do not make any prediction on the extent of the bistable domain in terms of stellar parameters, mass and rotation period . This issue shall be investigated by further theoretical work, and by surveys of activity and magnetism in the ultracool dwarf regime.

A dynamo bistability offers the possibility of hysteretic behaviour. Hence, the magnetic properties of a given object depend not only on its present stellar parameters, but also on their past evolution. For instance, for young objects, episodes of strong accretion can significantly modify their structure and hence the convective energy available to sustain dynamo action (Baraffe, Chabrier & Gallardo 2009); initial differences in rotation periods of young stars could also play a role. Because stellar magnetic fields are central in most physical processes that control the evolution of mass and rotation of young stars (in particular accretion–ejection processes and star–disc coupling, e.g. Bouvier 2009; Gregory et al. 2010), the confirmation of stellar dynamo bistability could have a huge impact on our understanding of the formation and evolution of low-mass stars.

ACKNOWLEDGMENTS

It is a pleasure to thank Katia Ferrière for helpful discussions and comments on this manuscript. We acknowledge the constructive comments of an anonymous referee.

REFERENCES

Baraffe I., Chabrier G., Gallardo J., 2009, ApJ, 702, L27
Bouvier J., 2009, in Neiner C., Zahn J.-P., eds, The Role of Magnetic Fields in Governing the Angular Momentum Evolution of Solar-type Stars. ESA, Noordwijk, p. 199
Browning M. K., 2008, ApJ, 676, 1262
Cattaneo F., Hughes D. W., 2009, MNRAS, 395, L48
Chabrier G., Baraffe I., 1997, A&A, 327, 1039
Chabrier G., Küker M., 2006, A&A, 446, 1027
Chandrasekhar S., 1961, Hydrodynamic and Hydromagnetic Stability. Clarendon, Oxford
Charbonneau P., MacGregor K. B., 1997, ApJ, 486, 502
Childress S., Soward A. M., 1972, Phys. Rev. Lett., 29, 837
Christensen U. R., Aubert J., 2006, Geophys. J. Int., 166, 97
Christensen U. R., Holzwarth V., Reiners A., 2009, Nat, 457, 167 (C09)
Cutri R. M. et al., 2003, 2MASS All Sky Catalog of Point Sources. The IRSA 2MASS All-Sky Point Source Catalog, NASA/IPAC Infrared Science Archive, http://irsa.ipac.caltech.edu/applications/Gator/
Delfosse X. et al., 2000, A&A, 364, 217
Donati J.-F., Brown S. F., 1997, A&A, 326, 1135
Donati J.-F. et al., 2003, MNRAS, 345, 1145
Donati J.-F. et al., 2006a, Sci, 311, 633
Donati J.-F. et al., 2006b, MNRAS, 370, 629
Donati J.-F. et al., 2008, MNRAS, 390, 545
Eltayeb I. A., Roberts P. H., 1970, ApJ, 162, 699
ESA, 1997, VizieR Online Data Catalog, 1239, 0
Fautrelle Y., Childress S., 1982, Geophys. Astrophys. Fluid Dyn., 22, 235
Featherstone N. A. et al., 2009, ApJ, 705, 1000
Goudard L., Dormy E., 2008, Europhys. Lett., 83, 59001
Gregory S. G. et al., 2010, Rep. Prog. Phys., 73, 126901
Kiraga M., Stepien K., 2007, Acta Astron., 57, 149
Morin J. et al., 2008a, MNRAS, 384, 77
Morin J. et al., 2008b, MNRAS, 390, 567
Morin J. et al., 2010a, MNRAS, 407, 2269 (M10a)
Morin J. et al., 2010b, preprint (arXiv:1009.2589)
Phan-Bao N. et al., 2009, ApJ, 704, 1721
Reiners A., 2010, preprint (arXiv:1012.1183)
Reiners A., Basri G., 2006, ApJ, 644, 497
Reiners A., Basri G., 2007, ApJ, 656, 1121
Reiners A., Basri G., 2010, ApJ, 710, 924
Reiners A., Basri G., Browning M., 2009, ApJ, 692, 538
Roberts P. H., 1978, in Roberts P. H., Soward A. M., eds, Rotating Fluids in Geophysics. Academic Press, London, p. 351
Roberts P. H., 1988, Geophys. Astrophys. Fluid Dyn., 44, 3
Rüdiger G., Kitchatinov L. L., Brandenburg A., 2011, Sol. Phys., 269, 3
Saar S. H., 1988, ApJ, 324, 441
Semel M., 1989, A&A, 225, 456
Simitev R. D., Busse F. H., 2009, Europhys. Lett., 85, 19001
Soward A. M., 1979, Phys. Earth Planet. Inter., 20, 134
St. Pierre M. G., 1993, in Proctor M. R. E., Matthews P. C., Rucklidge A. M., eds, Solar and Planetary Dynamos. The Strong Field Branch of the Childress-Soward Dynamo. Cambridge Univ. Press, Cambridge, p. 295
Stevenson D. J., 1979, Geophys. Astrophys. Fluid Dyn., 12, 139
Vitense E., 1953, Z. Astrophys., 32, 135
Vögler A., Schüssler M., 2007, A&A, 465, L43
Weiss N. O., Tobias S. M., 2000, Space Sci. Rev., 94, 99

This paper has been typeset from a TEX/LATEX file prepared by the author.